Regulative synthesis of capsular polysaccharides in the pathogenesis of *Streptococcus suis*

Xingye Wang[1], Jie Wang[1], Ning Li[1], Xin Fan[1], Beinan Wang[1#*]

[1]Key Laboratory of Pathogenic Microbiology and Immunology, Institute of Microbiology, Chinese Academy of Sciences, Beijing, China

[#]Address correspondence to Beinan Wang, wangbn@im.ac.cn

[*]Present address: No. 1 Beichen West Road, Chaoyang District, Beijing 100101, China.

Abstract

Streptococcus suis (*S. suis*) is an important zoonotic pathogen causing substantial economic losses in the swine industry. *S. suis* serotype 2 (SS2) is often isolated from the diseased. *S. suis* expresses capsular polysaccharide (CPS), a virulence factor crucial for their survival in the blood. However, the role of CPS in the pathogenesis of *S. suis* is incomplete. Here, we showed a dynamic regulation of CPS in *S. suis* pathogenesis. In a mouse infection model, an SS2 strain (05ZYH33) was detected in the nasal-associated lymphoid tissue (NALT) and cerebrospinal fluid (CSF) as early as 30 min after intranasal inoculation without bacteremia. Histological analysis revealed that 05ZYH33 in the nasal cavity invaded the olfactory epithelium, resulting in early brain inflammation. Transmission electron microscopy showed that 05ZYH33 isolated from NALT and CSF at early infection time had a thin layer of CPS, and those detected in the blood 5 h post-inoculation showed a much thicker CPS. In addition, adoptive transfer of anti-CPS restricted 05ZYH33 in the blood but not in NALT or CSF. However, an antiserum directed to multiple non-CPS virulence factors (anti-V5) efficiently inhibited 05ZYH33 in NALT, CSF, and blood. Thus, 05ZYH33 colonizes NALT more efficiently without CPS and subsequently invades the meninges through the olfactory nerve system. These findings provide valuable information for the treatment of *S. suis* infection and the development of vaccines across serotypes of *S. suis* by targeting CPS-independent immunity.

Keywords: *Streptococcus suis*, CPS, and meningitis.

Introduction

S. suis is a zoonotic pathogen in the porcine industry. Thirty-three serotypes of *S. suis* have been described to date based on the capsular polysaccharides (CPS). The *S. suis* serotype most frequently isolated from diseased swine and humans is serotype 2 (SS2). *S. suis* is commonly found in NALT of asymptomatic piglets. Under some unknown conditions, *S. suis* can reach and survive in the blood and invade the brain to cause meningitis and multi-organ dissemination. Infection of the central nervous system (CNS) is a cause of mortality in piglets with the disease. CPS is essential for survival of *S. suis* in the bloodstream and is recognized as an important virulence factor of this bacterial pathogen. However, the role of CPS in the pathogenesis of S. *suis* and the function of CPS-induced immunity in SS2 protection is controversial [1]. The opsonizing antibodies targeting CPS are protective [2, 3] but only partially protect against infection [4]. Furthermore, a CPS-glycoconjugated vaccine protected parenterally challenged piglets [5], but protection by anti-CPS has not been demonstrated in animals challenged through the intranasal route, which is a common natural infection route of *S. suis*.

Synthesis of CPS is enhanced in the bloodstream and reduced in the CNS [6, 7]. *In vitro* experiments revealed that the presence of CPS attenuated 05ZYH33 invasion of epithelial cells [8-10] and that unencapsulated mutants displayed increased rates of invasion of the blood–cerebrospinal fluid barrier (BCSFB) [8, 9]. These observations suggest that *S. suis* regulates CPS synthesis to fit hosts. However, despite the proposal of this hypothesis more than two decades ago, there is still no direct evidence of such encapsulation modulation for *S. suis* [11].

While CPS has been known for years and considered necessary for infection yet probably not sufficient, other surface-associated and secreted proteins of *S. suis* have received attention during the last years for their important virulent roles in the pathogenesis [3] and as vaccine candidates to raise effective immune response [15]. To cause disease, *S. suis* must colonize the respiratory mucosa, breach epithelial barriers, survive in the bloodstream, spread to different organs, and exaggerate inflammation. CPS and these virulent proteins contribute to the pathogenesis of the infection at specific steps.

Two pathways have been exploited by meningeal pathogens to access the CNS: penetrating the blood–brain barrier (BBB) or the BCSFB through the blood or directly accessing the CNS via the olfactory or trigeminal nerves [12]. Some human meningeal pathogens, such as *Streptococcus pneumoniae* and *Neisseria meningitidis*, can directly transmigrate from the nasal mucosa into the CNS through the olfactory nerve [12-14]. Similar to these meningeal pathogens, the predominant route of *S. suis* infection in pigs is through the upper respiratory tract (URT), which may provide the opportunity for *S. suis* to transmigrate directly to the CNS from the nasal cavity.

Studies on *S. suis* commonly use parenteral infection models that bypass colonization of the URT, thus this critical step of *S. suis* pathogenesis is largely unexplored. In the present study, mice were infected intranasally (i.n.) with 05ZYH33, and the infection process was monitored. We show that 05ZYH33 regulated the synthesis of CPS at different stages of infection and that 05ZYH33 migrated to the CNS from the nasal cavity independent of CPS before it entered the blood. Moreover, we revealed that immunity against non-CPS virulence factors of *S. suis* efficiently prevented nasal–CNS transmigration and subsequent progress of the infection.

Results

S. suis serotypes regulated CPS synthesis in different culture phases.

A clinical isolate of *S. suis* serotype 2 wild type (05ZYH33) was cultured and collected in the lag, logarithmic (log), and stationary phases [optical density at 600 nm (OD_{600}) of 0.20, 0.60, and 0.80, respectively] (Fig. 1A). The CPS of 05ZYH33 collected in different growth phases was quantitated based on hydrophobicity in a bacterial adhesion to hydrocarbon (BATH) assay. High surface hydrophobicity leads to high bacterial adherence to hydrocarbon (high BATH value) and reflects low levels of CPS on the surface of 05ZYH33. As shown in Fig. 1B, the CPS-deficient strain Δ2BSS2 (05ZYH33 isogenic), used as a control, exhibited the highest BATH value (69.5 ± 6.51%). A similarly high BATH value (62.5 ± 9.73%) was found in the log phase of 05ZYH33. However, the BATH values in the lag and stationary phases of 05ZYH33 were substantially lower (37.0 ± 17% and 15.6 ± 9.2%, respectively). These data indicate that CPS of 05ZYH33 was synthesized dynamically *in vitro*, with the highest quantity in the stationary phase and the lowest in the log phase.

To determine the dynamic CPS synthesis in *S. suis* serotypes, four other serotypes of *S. suis* were cultured and collected in the log and stationary phases for CPS quantitation by BATH assays. As shown in Fig. 1C, all the serotype strains had high hydrophobicity at the log phase and low at the stationary phase. The similarity in CPS patterns of these strains suggests a shared regulation mechanism by *S. suis* serotypes.

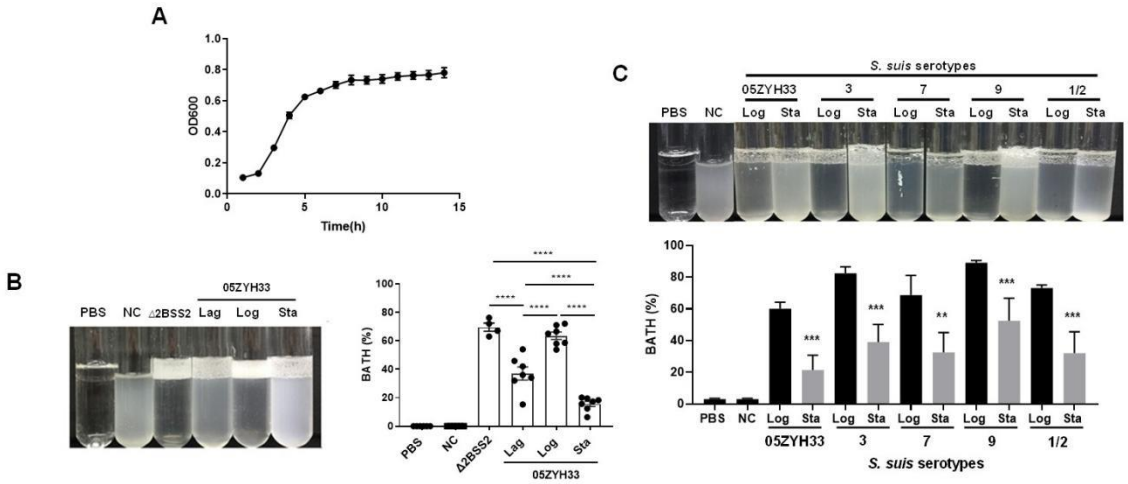

Monitoring the CPS content of *S. suis* serotypes in culture. (A) The growth curve of 05ZYH33 in TSB-FBS culture was assessed by measuring the optical density at 600 nm (OD600) at specified time points. Data present the mean ± SD of three independent experiments (n = 10). (B) The hydrophobicity of 05ZYH33 during the lag, log, and stationary (Sta) phases was measured by BATH assays (n = 4 to 7). (C) The hydrophobicity of indicated serotype strains in the log and stationary phases was measured by BATH assays. A representative photo of the BATH assay (upper panel) and BATH values (lower panel) (n = 3 to 6). Δ2BSS2 refers to an isogenic strain lacking CPS; NC represents a 05ZYH33 suspension without hydrocarbon. **, P <0.01. ***, P <0.001. ****, P <0.0001.

05ZYH33 in different cultural stages exhibited altered abilities for host cell adherence and resistance to bacterial killing.

05ZYH33 and Δ2BSS2 were cultured and collected at the log and stationary phases to determine the effects of CPS on the binding of 05ZYH33 to epithelial cells. The adherence assay showed that while 16.5 ± 5.2% of Δ2BSS2 was associated with epithelial cells (HEp-2), only 4.96 ± 3.26% of 05ZYH33 in the log phase and 2.05 ± 1.58% of 05ZYH33 in the stationary phase were associated with the cells (Fig. 2A). The bacterial binding was

Δ2BSS2 > 05ZYH33 in the log phase > 05ZYH33 in the stationary phase. Similar binding patterns of 05ZYH33 and Δ2BSS2 were also observed in the assay using human brain microvascular endothelial cells (hBMECs), the major component of the BBB (Fig. 2B). These results support that CPS reduces adherence of the bacteria to host cells.

CPS of *S. suis* plays a critical role in the resistance to bacterial killing. 05ZYH33 in different growth phases were co-incubated with the blood from naïve mice to determine the effect of CPS on bacterial killing. After incubation for 3 h, surviving bacteria in the blood examined by colony-forming units (CFUs) showed that substantially more 05ZYH33 in the log and stationary phases were detected compared with Δ2BSS2 in the matching growth phases. In addition, there were more surviving 05ZYH33 in the stationary phase compared with that in the log phase (Fig. 2C). These results suggest a correlation between lower CPS in the NALT and a greater capacity for cellular association, whereas elevated CPS levels in the blood are linked to improved resistance against bactericidal activity. However, the mechanisms behind these associations remain unknown.

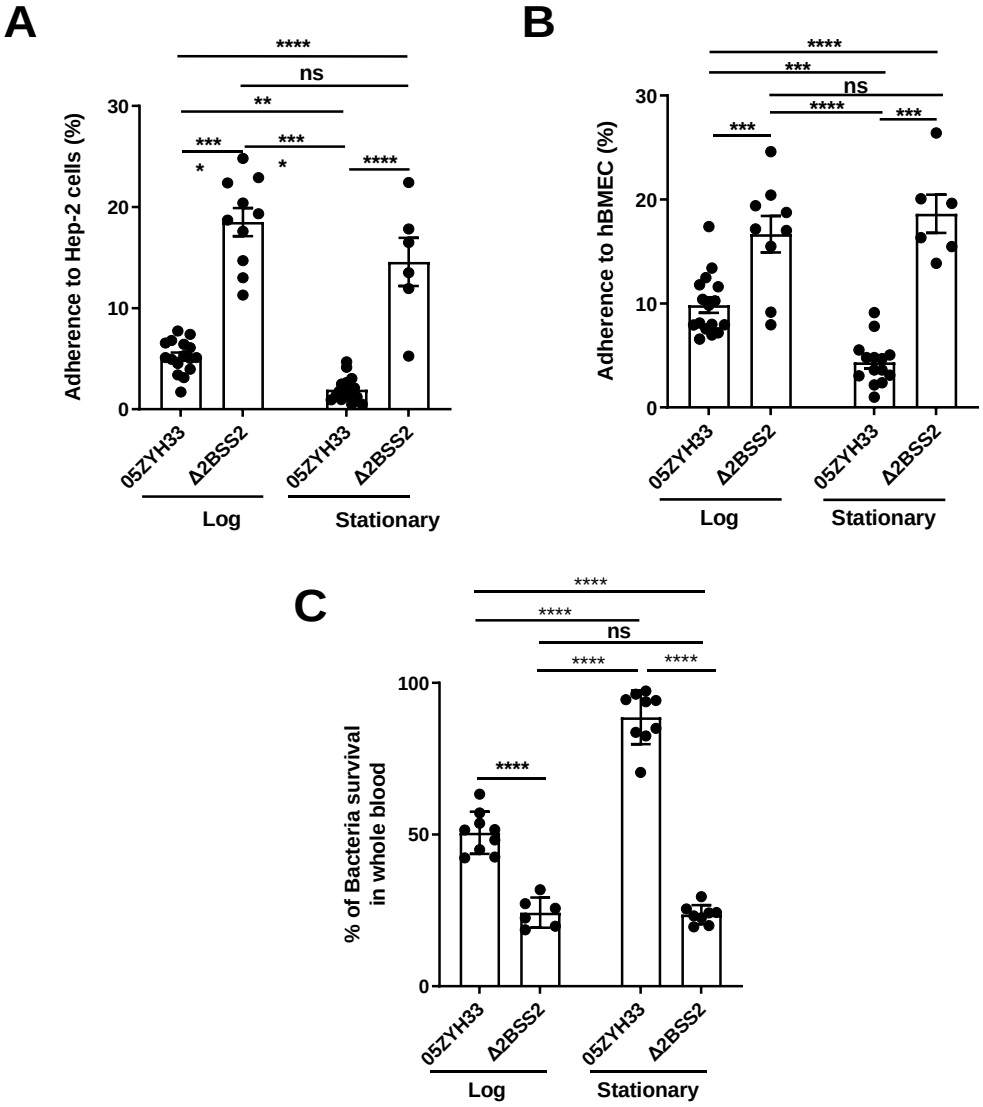

Fig. 2. The adherence of 05ZYH33 to epithelial cells and its resistance to bacterial killing. HEp-2 or HBMECs cells were inoculated with 05ZYH33 or Δ2BSS2 in either the log or stationary phase at an infection MOI of 10. (A) Adherence rate of *S. suis* to HEp-2 cells. (B) Adherence rate of *S. suis* to HBMECs. (C) *S. suis* strains in log and stationary phases were incubated with whole blood from naïve mice for 3 h, and the viability of *S. suis* was determined. Data are from three independent experiments and present as means ±

169 SEM (n = 6 to 16). **P <0.01, ***P <0.001, ****P <0.0001; ns, not significant.

170 **The course of 05ZYH33 infection in mice following intranasal inoculation.**

171 The dynamic synthesis of CPS associated with differential adherence to host cells and
172 resistance to bacterial killing *in vitro* suggested that 05ZYH33 regulates CPS synthesis for
173 pathogenesis and survival in a host. To determine the role of CPS dynamic synthesis in
174 05ZYH33 pathogenesis, mice were i.n. inoculated with 05ZYH33 to simulate *S. suis*
175 natural infection in pigs and CFUs in various bodily compartments were assessed at
176 different points over 120 h. By 0.5 h after inoculation, CFUs of 05ZYH33 in the nasal-
177 associated lymphoid tissue (NALT), a pig tonsil homologue and the major niche for *S. suis*
178 in pigs, and the lungs were similar (5×10^5) and gradually reduced with time (Figs. 3A and
179 3B), suggesting that the CFUs in the lungs are from the nasal cavity. Up to 10^5 CFUs were
180 also found in CSF samples by 0.5 h (Fig. 3C). The curves of CFUs in NALT, the lungs, and
181 CSF showed a similar trend, which was a high level for a few hours followed by a gradual
182 reduction with increasing days. In contrast, 05ZYH33 was not detected in the blood until
183 5.0 h after inoculation (Fig. 3D). As expected, CFUs in the spleen and heart at indicated
184 times (Figs. 3E and 3F) were similar to those in the blood, indicating that they disseminated
185 from the circulation. These findings suggested that 05ZYH33 in the nasal cavity can
186 transmigrate to the lungs and CNS before bacteremia and disseminate to other organs after
187 entering the blood. During the five days (120 h) following inoculation, the mice did not
188 show significant disease symptoms, and their physical conditions were similar compared
189 to non-infected mice (body weight, appetite, and activity). No obvious disease symptoms
190 might be due to the bacteria cleared relatively quickly.

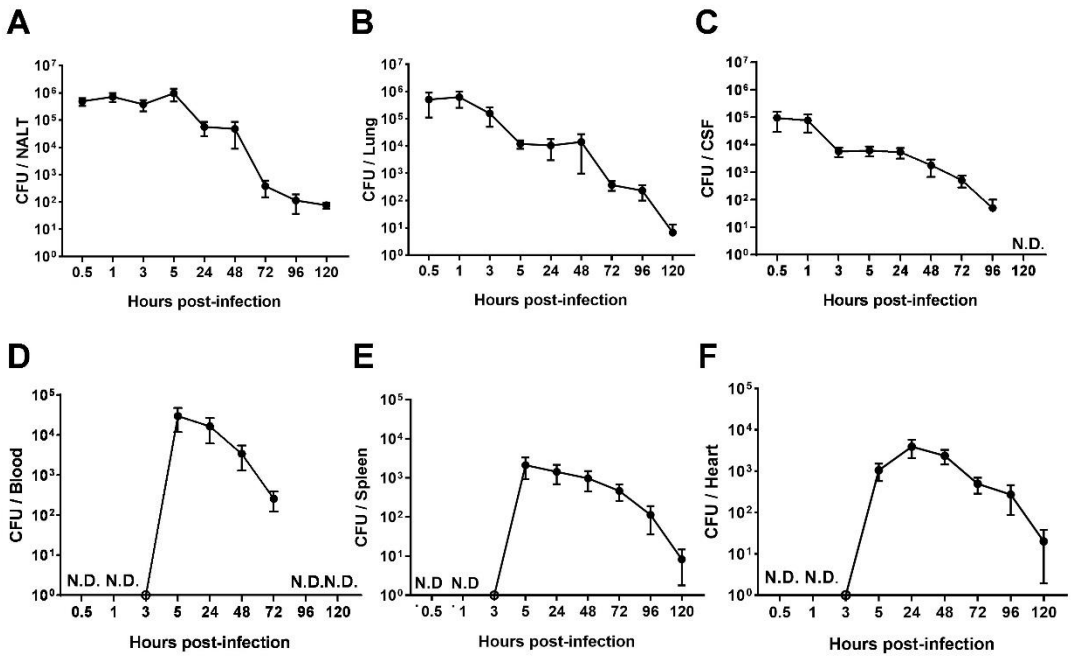

Fig. 3. The intranasal infection course in mice. Mice were intranasally inoculated with 05ZYH33. Total CFUs in various bodily compartments were assessed at the indicated time points after inoculation, (A) NALT, (B) the CSF, (C) the lung, (D) the blood, (E) the spleen, and (F) the heart. The data presented are derived from two independent experiments and presented as means ± SEM (n = 6). N.D., not detected.

The CPS of 05ZYH33 was synthesized differentially in stages of infection in mice.

05ZYH33 was isolated from the bodily compartments of mice 12 h after inoculation. The 12 h of infection allows the detection of the bacteria in different body compartments of the infected mice. Following enriched by culturing the isolates in TSB to an OD_{600} of 0.7 CPS synthesis *in vivo* was determined by BATH assay. The hydrophobicity of isolates from NALT and the CSF was lower compared with that of Δ2BSS2, but higher than that of the isolates from the blood (Fig. 4A). This indicates that 05ZYH33 downregulates CPS synthesis when it colonizes the nasopharyngeal mucosa or enters the CNS and upregulates CPS synthesis upon entering the blood. Transmission electron microscopy (TEM) was

206 performed directly on 05ZYH33 isolated from mice without *in vitro* culture to confirm the
207 BATH assay results. For cultured strains without mouse infection (Fig. 4Ba, b, and c),
208 similar to Δ2BSS2 (Fig. 4Ba), in the log phase (Fig. 4Bb) there was no CPS observed on
209 the dividing 05ZYH33 cell (left and larger cell) and only a thin and partial layer of CPS on
210 the smaller dividing cell (right, smaller cell) was observed. Whereas, a thicker layer of CPS
211 was observed on the surface of the bacteria in the stationary phase (Fig. 4Bc). For
212 05ZYH33 isolated directly from infected mice (Fig. 4Bd, e, and f), the CPS was much
213 thicker, denser, and uniformly distributed in the blood isolates (Fig. 4Bf) compared with
214 that of the NALT isolates where it was thinner and much sparser (Fig. 4Bd). In contrast,
215 the outermost layer of the isolates from the CSF was highly dense without an apparent CPS
216 layer (Fig. 4Be). These findings support that CPS downregulation is associated with
217 efficient colonization and upregulation with increased resistance to bacterial killing in the
218 blood.
219
220
221
222
223
224
225
226
227
228

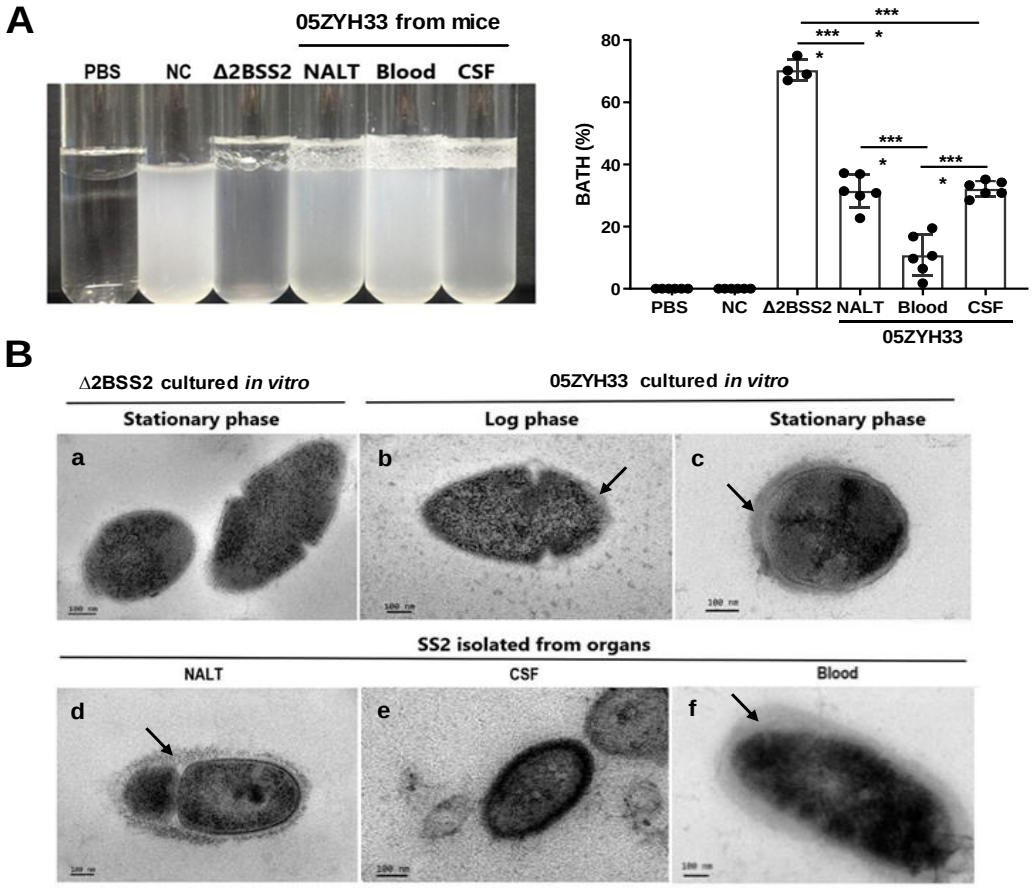

Fig. 4. The CPS of 05ZYH33 isolated from various bodily compartment following infection. 05ZYH33 was intranasally inoculated in mice. Twelve hour after inoculation, CFUs in NALT, the CSF, and the blood were assessed for (A) hydrophobicity of bacterial cells by BATH assay and (B) CPS by TEM. Arrows indicate the CPS layers. Scale bar, 100 nm. Data in (A) are from two independent experiments and present as means ± SEM (n = 4 to 6). NC, 05ZYH33 suspension without hydrocarbon. ****P <0.0001.

An antiserum against non-CPS virulence factors of *S. suis* reduced 05ZYH33 colonization in NALT, CSF, and lungs.

251 We have previously demonstrated that immunization with multiple non-CPS virulence
252 factors of *S. suis* (named V5) prevents 05ZYH33 colonization of the nasal mucosa and
253 neuropathological symptoms in mice [15]. We hypothesized that the serum against V5
254 would inhibit the nasal–CNS transmigration of 05ZYH33. Mice were i.n. infused with anti-
255 V5 or anti-CPS serum, inoculated i.n. with 05ZYH33 6 h later, then euthanized 12 h post-
256 inoculation (Fig. 5A) to detect the bacteria in different body compartments of the infected
257 mice. In mice that received antisera through the i.n. route, CFUs reduced in all examined
258 compartments of anti-V5 recipients but only reduced in the lungs and blood of anti-CPS
259 recipients (Fig. 5B). These results indicated that 05ZYH33 survival in the blood depends
260 on CPS and nasopharyngeal colonization and nasal–CNS transmigration are more
261 dependent on non-CPS molecules of 05ZYH33. In addition, when mice received either
262 anti-V5 or anti-CPS through the intravenous (i.v.) route, CFUs were reduced in the lungs
263 and blood but not in NALT and the CSF (Fig. 5C), compared with mice received naïve
264 serum through the i.v. route. These observations suggest that systemic immunity could
265 efficiently protect against infection in the lungs and blood but not against colonization in
266 the nasal mucosal and CNS, at least at the early infection time.

267 The simultaneous 05ZYH33 colonization in NALT and CNS support a nasal–CSF
268 transmigration. To exclude the possibility that CFUs in the CNS at 12 h post-infection is
269 disseminated from the circulation, mice received antisera via the i.n. route and were
270 inoculated with 05ZYH33 as before, then CFUs were determined 1 h post-inoculation
271 before the bacteria entered the blood (Fig. 5A). As shown in Fig. 5D, CFUs in NALT and
272 the CSF of anti-CPS recipients were similar to those in naïve-serum recipients; however,
273 those in NALT and the CSF of anti-V5 recipients were 10-fold lower compared with those

of the naïve-serum recipients. To confirm that the nasal–CNS transmigration is independent of CPS, mice received naïve serum or anti-V5 via the i.n. route, then were inoculated with Δ2BSS2. One hour later, we found 4.5 x 10^5 CFUs in NALT and 2.1×10^5 CFUs in the CFS of naïve-serum recipients. However, CFUs were 10-fold and 100-fold lower in NALT and the CSF, respectively, of anti-V5 recipients compared with those in naïve-serum recipients (Fig. 5E). These results demonstrate that 05ZYH33 in the CNS in the early infection is from the nasal cavity independent of CPS.

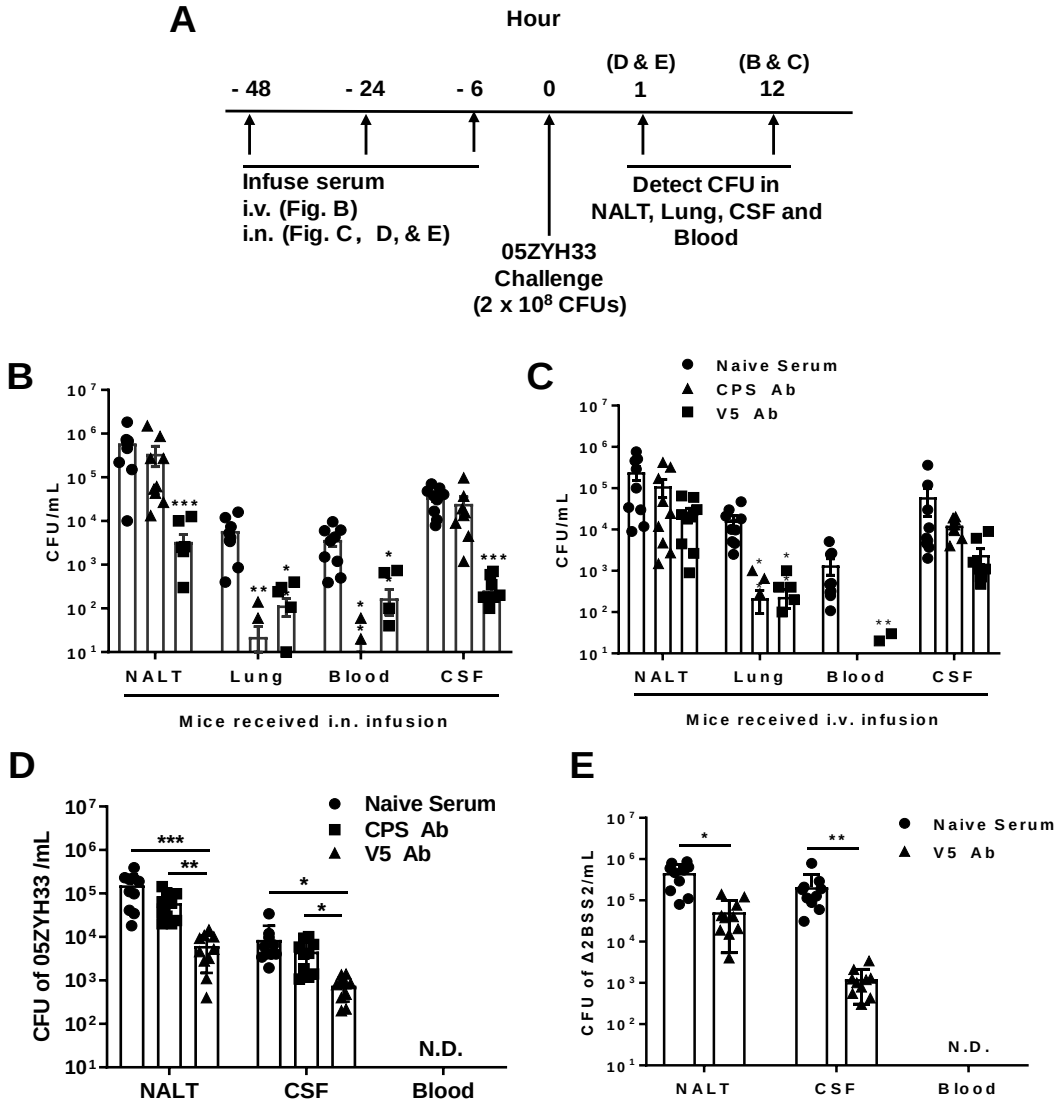

Fig. 5. The role of anti-CPS or anti-V5 serum in 05ZYH33 infection. (A) Schematic illustration of passive transfer of antisera and infection in mice. (B) and (C) Anti-V5 or ant-CPS antiserum was transferred through the i.n. or i.v. route. Six hours later, mice were i.n. challenged with 05ZYH33, then euthanized 12 h post-challenge. CFUs of 05ZYH33 in NALT, the lungs, the blood, and the CSF were determined. (D) and (E) Mice were infused with anti-V5 or anti-CPS serum through the i.n. route, and inoculated i.n. with 05ZYH33 or Δ2BSS2 6 h later. One hour later, mice were euthanized, and CFUs in NALT, the blood, and the CSF were determined. Data are the mean ± SEM of three independent experiments (n = 9 - 10). *P <0.05, **P <0.01, ***P <0.001.

The olfactory nerve is the invasion route of 05ZYH33 for nasal–CNS transmigration.

The olfactory nerve is a port of entry to the meninges for some human meningeal pathogens and is the likely the route of the early CNS dissemination by 05ZYH33. One hour after infection, the mice were sacrificed, and their heads were sectioned and stained for histological analysis. Figure 6A presents a histological overview of the anatomical structures the distal NC and OB regions, while Figure 6B illustrates the locations of the anatomical compartments in the area. The tissue section showed that compared with uninfected mice (Fig. 6A, *a*, *c,* and *e*), Scattered and grouped bacteria were observed on the surface of and in the olfactory epithelium (OE) (Fig. 6A*, b,* and *d*, orange signal, arrowheads), accompanied by severely destroyed tissue (indicated by the loss of immunofluorescence signal in the area) (Fig. 6A*, d*). Large groups of bacteria were observed within the olfactory bulb (OB) (Fig. 6A, *f*). These observations suggest that 05ZYH33 in the nasal cavity could invade the olfactory epithelium through the sensory neurons protruding into the NC and subsequently enter the brain along the sensory neurons

320 at the cribriform plate. Histological analysis of the brain in 05ZYH33-infected mice
321 revealed that inflammatory cells were infiltrated in the distal part of the brain tissue with
322 surrounding edema at 1 h post-inoculation (Fig. 6C, *c* and *d*). The pathological changes
323 were more severe 9 days after 05ZYH33 inoculation (Fig. 6C, *e* and *f*). Since CSF flows
324 into the subarachnoid space of the spinal cord and around the brain [16, 17] the distal
325 inflammation is consistent with the brain's anatomical structure. Thus, nasal–CNS
326 transmigration is an efficient route of *S. suis*-mediated CNS infection.

327 Mice were pretreated with acetic acid to increase the sensitivity to 05ZYH33 infection
328 [15]. To exclude that nasal-CNS transmigration results from irritation of the
329 nasopharyngeal mucosa by acetic acid, mice were infected without acid treatment
330 (pretreated with PBS). One hour post-inoculation CFUs were found in the CSF of the mice
331 even though the numbers were lower than those of acidic acid-treated mice (Fig. 6D). CFUs
332 were also detected in the CSF when mice were infected with Δ2BSS2 without acid
333 treatment (Fig. 6E). These results indicated that nasal-CSF transmission takes place
334 without acidic acid and independent of CPS and that irritation of the nasopharyngeal
335 mucosa facilitates nasal-CNS transmission.

336

337

338

339

340

341

342

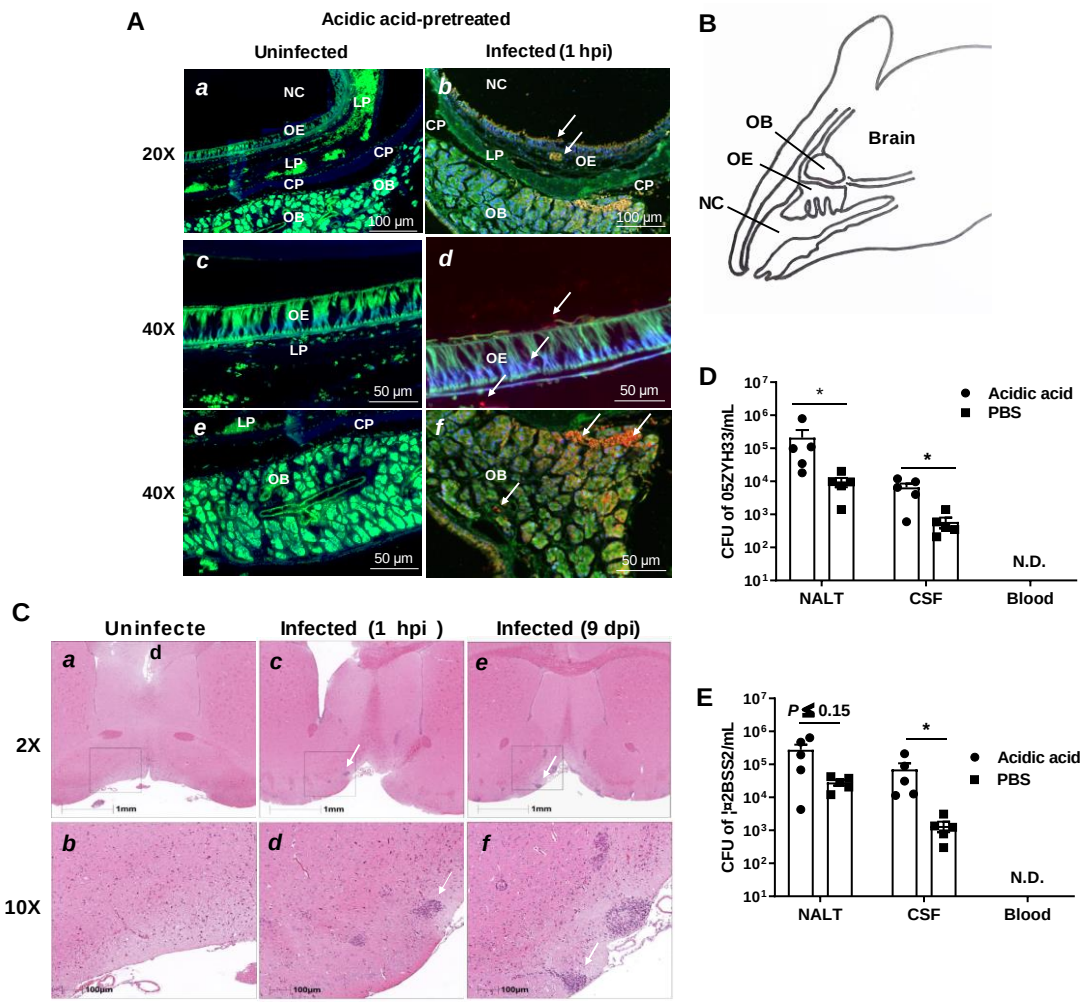

Fig. 6. Detection of the presence of 05ZYH33 in the tissue of olfactory nerve area. Mice were inoculated with acetic acid through the nostril and one hour later infected i.n. with 05ZYH33. (A) Sagittal views of the olfactory system. Sections of the distal nasal cavity and olfactory epithelium from uninfected (*a*, *c*, and *e*) and 05ZYH33-infected (*b*, *d*, and *f*) mice. Red or orange, 05ZYH33; green, the neuronal marker β-tubulin III; blue, DNA. NC, Nasal cavity; OE, olfactory epithelium; LP, lamina propria; CP, cribriform plate; OB,

olfactory bulb. (B) A draw of the sagittal plane of the rodent nose elucidates the compartments of the olfactory bulb (OB), olfactory epithelium (OE), nasal cavity (NC), and the braian. (C) One hour or nine days after 05ZYH33 infection, the brain of mice were sectioned for H&E staining. Arrows indicate infiltrated inflammatory cells. (D) and (E) Mice were inoculated with acetic acid or PBS and one hour later infected i.n. with 05ZYH33 or Δ2BSS2. (D) CFUs of 05ZYH33 or (E) Δ2BSS2 in NALT, the CSF, and blood were determined one h after infection.

Discussion

CPS is an important virulence factor of *S. suis*, but its role in *S. suis* pathogenesis is controversial. Most animal models in studies of *S. suis* employ the intraperitoneal (i.p.) or i.v. route for infection, which bypass the nasopharynx, the natural infection route of *S. suis*. In this study, CPS thickness of *S. suis* SS2 strain 05ZYH33 was monitored in an i.n. infection mouse model. The results indicate that that *S. suis* CPS can be dynamically synthesized during the development of the bacterial infection. We showed that the downregulation of CPS synthesis by 05ZYH33 is associated with increased nasopharyngeal colonization and early nasal–CNS transmigration before bacteremia. This is consistent with previous studies that showed the upregulation of CPS is related to increased resistance to bacterial killing later in the blood. The study also indicates that CPS-independent immunity can prevent nasal–CNS transmigration and the progression of 05ZYH33 infection.

Clinical CNS symptoms in pigs are often preceded by a phase of bacteremia [16, 17], indicating that *S. suis* meningitis results from the dissemination of bacteria from the blood through the BBB or the blood–CSF barrier. Our study revealed that, like some human

389 meningeal pathogens, the olfactory nerve epithelium provides an alternative route for
390 05ZYH33 invasion to the CNS. Swine influenza virus (SIV) infection was reported to
391 promote *S. suis* invasion of deeper tissues by damaging epithelial cells [18-20].
392 Nasopharyngeal inflammation by co-infected *S. suis* and SIV could cause tissue damage to
393 the olfactory epithelium, which may exacerbate nasal–CNS entry. As the mouse is not a
394 natural host of *S. suis* and is insensitive to the infection, a relatively high dosage is needed
395 for optimal bacterial retention in NALT, which can lead bacteria into the lungs. Thus, early
396 05ZYH33 colonization in the lungs of this model may not reflect the state of *S. suis*
397 infections in pigs. The early 05ZYH33 colonization in NALT and the CSF with similar
398 dynamics suggests that meningitis could be early manifestations of *S. suis* disease before
399 multi-organ dissemination through the blood. The findings in the study indicate that
400 restriction of *S. suis* proliferation in NALT is critical to prevent the severity and lethality
401 of *S. suis* disease.

402 We noticed that the outermost layer of the isolates from the CSF was highly dense
403 without an apparent CPS layer (Fig. 4Be), suggesting that other membrane components of
404 the CSF isolates are also changed besides CPS. It is unclear whether this change is related
405 to CSF colonization and what molecules have changed. Although CPS plays an important
406 role in *S. suis* survival in the blood, it is not the only component required for the event [21,
407 22]. Similar to that observed with anti-CPS, infusion of anti-V5 through the i.v. route
408 reduced 05ZYH33 in the blood and lungs, indicating that blocking CPS-independent
409 mechanisms can restrain the progression of 05ZYH33 infection and suggests that non-CPS
410 virulence factors, such as those in V5, are required for 05ZYH33 survival in the blood and
411 lungs. Furthermore, although anti-CPS promoted 05ZYH33 clearance in the blood, it did

not prevent 05ZYH33 colonization of the nasal cavity and invasion of the CNS. However, anti-V5 reduced 05ZYH33 in all examined compartments when administered via the i.n. route, supporting that inhibition of nasal colonization by CPS-independent immunity is critical to prevent the progression of the disease. Moreover, the nasal-CNS route may not be the main pathway for clinical meningitis compared to the blood-CNS route. However, mucosal blockage of nasal colonization reduces CFU in the CSF more effectively than systemic antibody, indicating reduction of nasal colonization at early time would significantly prevent the bacteria from entering the CNS through the early nasal and later blood route.

In summary, this study supports an updated *S. suis* infection model. Briefly, 05ZYH33 downregulates CPS to colonize the URT mucosa, where it can transmigrate to the CNS through the olfactory epithelium early in the infection process. 05ZYH33 upregulates CPS to avoid bacterial killing when it enters the blood, leading to multi-organ dissemination. The regulation of CPS at different stages of 05ZYH33 pathogenesis and the protection offered by CPS-independent immunity provide valuable information for clinical treatment and development of vaccines across serotypes of *S. suis*.

Materials and methods

Ethics statement

This study was performed in strict accordance with the recommendations in the Guide for the Care and Use of Laboratory Animals of the IMCAS (Institute of Microbiology, Chinese Academy of Sciences) Ethics Committee. The protocol was approved by the Committee on the Ethics of Animal Experiments of IMCAS (permit no. APIMCAS2019004). Mice were bred under specific pathogen-free (SPF) conditions in the

435 laboratory animal facility at IMCAS. All animal experiments were conducted under
436 isoflurane anesthesia, and all efforts were made to minimize suffering.

437 **Bacterial strains and growth conditions**

438 *S. suis* strain SS2 05ZYH33 (GenBank no. for complete genome sequence:
439 CP000407.1) was isolated from a fatal human case of streptococcal toxic shock-like
440 syndrome (STSLS) in 2005 in Sichuan province, China. A capsular mutant of *S. suis*
441 05ZYH33 (Δ2BSS2) was obtained from Prof. Jia-Qi Tang (General Hospital of the Eastern
442 Theater of the People's Liberation Army, China) [23]. *S. suis* serotypes SS3, SS7, SS9, and
443 SS1/2 were gifts from Dr. Shengbo Cao (National Key Laboratory of Agricultural
444 Microbiology, Huazhong Agricultural University, Wuhan, China). The information of these
445 strains is listed in Supplementary Table 1. All *S. suis* strains were cultured in tryptic soy
446 broth (TSB) containing 5% newborn bovine serum (FBS) or on tryptic soy agar (TSA)
447 supplemented with 5% FBS at 37°C and 5% CO_2. The cultured strains were washed and
448 resuspended in phosphate-buffered saline (PBS). CFUs were verified by plating on blood
449 agar.

450 **Growth curve of 05ZYH33**

451 05ZYH33 was grown in TSB-FBS medium to an OD_{600} of approximately 0.4 and then
452 diluted 1000 times with fresh medium. Next, 200 μL of the bacterial suspension was added
453 in quadruplicate to a 100-well honeycomb plate and cultured at 37°C and 5% CO_2 for 16
454 h. The OD_{600} of each well was measured at different times using a CMax Plus plate reader
455 (Molecular Devices, San Jose, CA, USA).

456 **Determination of CFUs in various bodily compartments**

457 Mice were infected i.n. with 05ZYH33 (stationary phase). Then at different time

points, the lung, spleen, heart, and NALT were taken from mice, and the blood and CSF were collected. A single-cell suspension of each organ was prepared in 1-5 mL PBS. CFUs in the single cell suspension, the blood, and the CSF were determined by plating serially diluted samples on blood agar plates and expressed as total CFUs in each organ or in the blood and CFS by following formula: CFUs on the plate x dilution factor x total volume of a sample.

Bacterial adhesion to hydrocarbon (BATH) assay

The hydrophobicity of *S. suis* was assessed by a modified BATH assay [24]. Briefly, 05ZYH33 cells in cultures were collected, washed, and resuspended in PBS, adjusting the OD_{600} of the suspensions to 2.0 (±0.2) with PBS. Four milliliters of each suspension were added to a tube containing 300 μL xylene and 300 μL hexadecane. A negative control comprised a 4 mL bacterial suspension without hydrocarbon. After vortexing for 20 s, the tubes were maintained at 37°C for 30 min. The OD_{600} of the resulting lower aqueous layer and the tube contents before vortexing were measured. The ratio of the absorbance of the bacteria assay tubes (Ab) to the absorbance of the bacteria control (Ac) was calculated as adhesion to hydrocarbon (%) = (Ac − Ab) / Ac × 100.

Bacterial adherence assay

The human laryngeal epithelial cells (HEp- 2, CL-0104) were purchased from Procell Life Science &Technology Co., Ltd. Wuhan, Hubei Province and cultured according to the manufacturer's instruction. The human brain microvascular endothelial cells (hBMEC) were kindly provided by Prof. Xiang-Ru Wang in Huazhong Agricultural University, Wuhan, Hubei, China and cultured as described by Yang [25]. Adherence of 05ZYH33 or Δ2BSS2 in log and stationary phases was performed as described previously with slight

modifications [26]. Cells were cultured in 24-well plates to 80–90% confluence (~1.2 × 10^5 cells/well), then starved overnight in DMEM without serum and antibiotics. Cell monolayers were washed with PBS and overlaid with DMEM medium with 10% FBS (500 μL/well) containing 05ZYH33 or Δ2BSS2 (MOI = 10). After incubation for 2 h at 37℃ and 5% CO_2, unbound bacteria were removed, and the cells were lysed with 0.025% Triton X-100. CFUs in samples of diluted cell lysate were determined on blood agar plates and expressed as the percentage of adherence: (CFUs in wells with cells / CFUs in wells without cells) × 100.

Bactericidal assay

Bactericidal assays were performed as described by Pian et al. [27] with slight modifications. Briefly, 1 × 10^5 05ZYH33 or Δ2BSS2 in log and stationary phases were added to whole blood from naïve mice. The mixtures were rotated for 3 h at 37°C and 5% CO_2. A set of the same bacterial samples was added to naive serum to determine bacterial numbers in the 3 h incubation without killing. Viable bacterial counts were determined by plating diluted samples on blood agar. The anti-killing capacity was calculated as (CFU in blood / CFU in serum) × 100%.

Mouse infection

C57BL/6JCnc wild-type mice (aged 6 to 7 weeks) were purchased from Vital River Laboratory Animal Center (Beijing, China) and randomly assigned to groups. Mice were pretreated with 5 μL of 1% acetic acid (pH 4.0) or PBS per nostril 1 h before intranasal infection [15]. After further anesthesia, mice were inoculated intranasally with 05ZYH33 (stationary phase, 2 × 10^8 CFU / 10 μL). 5 μL of the inoculum was delivered intranasally to each nostril (total 10 μL). This volume allows optional bacterial retention in NALT.

504 **Specimen collection and preparation**

505 Mice were euthanized, then blood samples were collected from the heart, and the
506 lungs, heart, spleen, and NALT were removed and washed with PBS to eradicate blood
507 contamination. Single-cell suspensions of the tissues were prepared by mechanical
508 dissociation of tissue through a 100-μm nylon mesh in 1 mL PBS. For CSF collection, the
509 nose part was removed from the head along the line of the eyeballs after the collection of
510 NALT tissue. The brain tissue was taken from the remaining part of the head and soaked
511 in 1 mL PBS for 1 h after sufficient laceration to expose the subarachnoid space without
512 mincing. This operation avoided damaging the integrity of brain tissue as much as possible.
513 Supernatants of the single-cell suspension and the blood and CSF samples were used to
514 detect CFU and examine the CPS.

515 **Transmission electron microscopy (TEM)**

516 *S. suis* cells were enriched by gradient centrifugation of homogenized NALT and
517 samples of the blood and CSF of infected mice. After washing, the bacteria were fixed in
518 2% paraformaldehyde supplemented with 0.05% ruthenium red in 0.1 M phosphate buffer
519 (pH 7.0) for 30 min at room temperature. The bacterial samples were further prepared and
520 embedded in epoxy resin (Epon 812, Merck) as described by Bojarska et al. [28]. Ultrathin
521 (70−80 nm) sections were cut, stained with 1.2 % uranyl acetate and 2.5 % lead citrate, and
522 then examined with a JEM-1400 (120 kV) transmission electron microscope (JEOL, Tokyo,
523 Japan). Images were taken with a Morada digital camera (Olympus SIS, Mŭnster, Germany)
524 at 10 M pix resolution.

525 **Cloning and expression of recombinant V5 proteins**

526 V5 contains five conserved virulence factors of *S. suis*. They are SrtA (amino acids 50

527 to 249), ScpCL (amino acids 36 to 535), MRP (amino acids 283 to 721), SLY (amino acids
528 28 to 497), and SspA (amino acids 41 to 852) and prepared as described by Xing X. et al.
529 (15). Briefly, the genes of V5 were cloned from the genome of *S. suis* strain A7 (serotype
530 2) (GenBank accession number: NC_017622.1). The recombinant proteins of V5 were
531 expressed in E. coli BL21 (DE3) and purified by immobilized metal ion affinity
532 chromatography (IMAC) to reach 95% purity. Bacterial lipopolysaccharide was removed
533 following purification (≤ 0.1 EU/μg). Protein concentrations were determined using the
534 BCA Protein Assay Kit according to the manufacturer's instructions (TIANGEN, catalog
535 number: PA115-02).

536 **Preparation and purification of anti-CPS and anti-V5 antibodies**

537 A female New Zealand white rabbit (SPF, 2.0–2.5 kg) was purchased from JinMuYang
538 Laboratory Animal Center (Beijing, China) and kept in the SPF animal facility for 1 week.
539 V5 (1 mg) was mixed with 1 mL incomplete Freund's adjuvant (Becton Dickinson,
540 Franklin Lakes, NJ, USA) and subcutaneously injected into the rabbit 4 times at 1-week
541 intervals. Blood samples were harvested 10 days after the last immunization, and the serum
542 was isolated. Anti-CPS (anti-*S. suis* serotype 2) serum was purchased from SSI Diagnostica
543 (Hillerød, Denmark) and purified by absorption with V5 by Ni-NTA agarose (Qiagen,
544 catalog no. 30210) according to the manufacturer's instructions. Briefly, 200 μL of V5
545 (His-tagged, 1 μg/μL) were loaded on the 5 mL Ni-NTA agarose column. The collected
546 antiserum was further purified by incubation with formalin-inactivated Δ2BSS2 (5×10^{10}
547 CFU) overnight at 4°C. The purified anti-CPS recognized 05ZYH33 but not Δ2BSS2 as
548 determined by enzyme-linked immunosorbent assay (ELISA) against 05ZYH33 and
549 Δ2BSS2, respectively. Titers of the purified antisera against V5 and CPS were evaluated

550 by ELISA and stored at −80°C until use.

551 **Passive antiserum transfer**

552 Female C57BL/6JCnc mice (6–8 weeks) were transferred with anti-CPS or anti-V5
553 serum through the i.n. or i.v. route. Optimal amounts of antisera were predetermined in
554 mouse infection assays (the minimum amount of anti-V5 to inhibit 05ZYH33 colonization
555 in NALT and the minimum amount of anti-CPS to prevent bacteremia). For anti-CPS serum,
556 20 μg/200 μL (100 μg/mL) was used for tail vein injection or 5 μg/30 μL (170 μg/mL) for
557 nasal drip. For anti-V5 serum, 100 μg/200 μL (500 μg/mL) and 50 μg/30 μL (170 μg/mL)
558 were used through the i.v. and i.n. routes, respectively. Six hours after antiserum transfer,
559 mice were inoculated via the i.n. route with 2×10^8 CFU of 05ZYH33, and CFUs in
560 different compartments of the infected mice were determined.

561 **Immunofluorescence staining and confocal microscopy**

562 Immunofluorescence staining and confocal microscopy of the nasal cavity were
563 performed as described by Pagelow et al. [29]. Briefly, whole heads of the mice were fixed
564 with 4% PFA for at least 24 h before embedding in paraffin wax. Sections of longitudinally
565 bisected heads were deparaffinized followed by antigen retrieval. Immunostaining was
566 conducted using a primary rabbit anti-*S. suis* antibody (1:100) and a mouse anti-tubulin
567 beta III antibody (Merck Millipore, Darmstadt, Germany catalog no. mab5564, 1:300) to
568 detect neuronal structures, and then appropriate fluorophore-conjugated secondary
569 antibodies: donkey anti-rabbit Cy3 (Jackson Immuno-Research Laboratories, Ely, United
570 Kingdom, catalog no. 711-166-152, 1:1000), donkey anti-mouse FITC (Jackson
571 ImmunoResearch Laboratories, Ely, United Kingdom, catalog no. 715-096-150, 1:500).
572 Tissues were mounted with Vectashield Mounting Medium with DAPI (Vector

573 Laboratories, Burlingame, CA, USA. catalog no. H-1200). Images were captured using a
574 Leica Aperio Versa 200 scanning microscope and color-balanced uniformly across the field
575 of view using the Image Processing Leica Confocal and ImageJ Software (Wayne Rasband,
576 National Institutes of Health, Bethesda, MD, USA).

577 **Histological analysis of brain tissue**

578 Mice were treated with 5 μL of 1% acetic acid (pH 4.0) per nostril. One hour later,
579 one group of mice was inoculated i.n. with 05ZYH33 (2×10^8 CFU). A control group of
580 mice was given PBS via the i.n. route. Infected mice were euthanized 1 h and 9 days after
581 infection, respectively. The brain was removed and quickly fixed with 4%
582 paraformaldehyde. After paraffin embedding, tissue sections were stained with
583 hematoxylin and eosin (H&E) according to a standard protocol and examined using a Leica
584 SCN400 slide scanner (Leica Microsystems, Germany).

585 **Statistical analysis**

586 Statistical analyses were performed in GraphPad Prism software, version 7.0. CFUs
587 were analyzed by two-tailed unpaired Mann–Whitney U nonparametric *t*-tests. An
588 unpaired, two-tailed Student's *t*-test was used to analyze the statistical significance
589 between two groups. One-way analysis of variance (ANOVA) with Tukey's post-hoc test
590 was used to analyze the statistical significance of differences among more than two groups.
591 A *P*-value of <0.05 was considered significant.

592 **Acknowledgments**

593 The authors acknowledge Prof. Jiaqi Tang of General Hospital of the Eastern Theater
594 of the People's Liberation Army of China for providing the capsular mutant of *S. suis*
595 05ZYH33 (Δ2BSS2), Dr. Shengbo Cao (National Key Laboratory of Agricultural

Microbiology, Huazhong Agricultural University, Wuhan, China) for sharing *S. suis* serotype strains, Prof. Xiang-Ru Wang in Huazhong Agricultural University, Wuhan, Hubei, China for the human brain microvascular endothelial cells (hBMEC), and Dr. Junfeng Hao in Pathological Laboratory of Institute of Biophysics, CAS, for performing the immunofluorescence microscopy. This research was supported by the National Natural Science Foundation of China grant 31872743 (to B.W.) and the China Postdoctoral Science Foundation Grant 2019M650875 (to X. W.).

Author contributions

B.W. conceived the original idea, designed the experiments and wrote the manuscript. X.W. performed the experiments, analyzed the data, and drafted the manuscript. J.W., N.L., and X.F. contributed to mouse experiments and provided advice on experimental designs.

Competing interests

The authors declare no competing interests.

References

1. Lun ZR, Wang QP, Chen XG, Li AX, Zhu XQ. Streptococcus suis: an emerging zoonotic pathogen. Lancet Infect Dis. 2007;7(3):201-209. doi: 10.1016/S1473-3099(07)70001-4.
2. Smith HE, Damman M, van der Velde J, Wagenaar F, Wisselink HJ, Stockhofe-Zurwieden N, et al. Identification and characterization of the CPS locus of Streptococcus suis serotype 2: the capsule protects against phagocytosis and is an important virulence factor. InfectImmun. 1999;67(4):1750-1756. doi: 10.1128/IAI.67.4.1750-1756.1999.
3. Fittipaldi N, Segura M, Grenier D, Gottschalk M. Virulence factors involved in the

pathogenesis of the infection caused by the swine pathogen and zoonotic agent Streptococcus suis. Future Microbiol. 2012;7(2):259-279. doi: 10.2217/fmb.11.149.

4. Charland N, Jacques M, Lacouture S, Gottschalk M. Characterization and protective activity of a monoclonal antibody against a capsular epitope shared by Streptococcus suis serotypes 1, 2 and 1/2. Microbiology (Reading). 1997; 143(Pt11):3607-3614. doi: 10.1099/00221287-143-11-3607.
5. Goyette-Desjardins G, Lacouture S, Auger JP, Roy R, Gottschalk M, Segura M. Characterization and Protective Activity of Monoclonal Antibodies Directed against Streptococcus suis Serotype 2 Capsular Polysaccharide Obtained Using a Glycoconjugate. Pathogens. 2019; 8(3):139. doi: 10.3390/pathogens8030139.
6. Wu Z, Wu C, Shao J, Zhu Z, Wang W, Zhang W. The Streptococcus suis transcriptional landscape reveals adaptation mechanisms in pig blood and cerebrospinal fluid. RNA. 2014;20(6):882-898. doi: 10.1261/rna.041822.113.
7. Willenborg J, Fulde M, de Greeff A, Rohde M, Smith HE, Valentin-Weigand P, et al. Role of glucose and CcpA in capsule expression and virulence of Streptococcus suis. Microbiology (Reading). 2011;157(Pt 6):1823-1833. doi: 10.1099/mic.0.046417-0.
8. Schwerk C, Papandreou T, Schuhmann D, Nickol L, Borkowski J, Steinmann U, et al. Polar invasion and translocation of Neisseria meningitidis and Streptococcus suis in a novel human model of the blood-cerebrospinal fluid barrier. PLoS One. 2012;7(1):e30069. doi: 10.1371/journal.pone.0030069.
9. Tenenbaum T, Papandreou T, Gellrich D, Friedrichs U, Seibt A, Adam R, et al. Polar bacterial invasion and translocation of Streptococcus suis across the blood-cerebrospinal fluid barrier in vitro. Cell Microbiol. 2009;11(2):323-336. doi:

10.1111/j.1462-5822.2008.01255.x.

10. Benga L, Goethe R, Rohde M, Valentin-Weigand P. Non-encapsulated strains reveal novel insights in invasion and survival of Streptococcus suis in epithelial cells. Cell Microbiol. 2004;6(9):867-881. doi: 10.1111/j.1462-5822.2004.00409.x.

11. Gottschalk M, Segura M. The pathogenesis of the meningitis caused by Streptococcus suis: the unresolved questions. Vet Microbiol. 2000;76(3):259-272. doi: 10.1016/s0378-1135(00)00250-9.

12. Dando SJ, Mackay-Sim A, Norton R, Currie BJ, St John JA. Pathogens penetrating the central nervous system: infection pathways and the cellular and molecular mechanisms of invasion. Clin Microbiol Rev. 2014;27(4):691-726. doi: 10.1128/CMR.00118-13.

13. van Ginkel FW, McGhee JR, Watt JM, Campos-Torres A, Parish LA, Briles DE. Pneumococcal carriage results in ganglioside-mediated olfactory tissue infection. Proc Natl Acad Sci USA. 2003;100(24):14363-14367. doi: 10.1073/pnas.2235844100.

14. Sjölinder H, Jonsson AB. Olfactory nerve--a novel invasion route of Neisseria meningitidis to reach the meninges. PLoS One. 2010;5(11):e14034. doi: 10.1371/journal.pone.0014034.

15. Xing X, Bi S, Fan X, Jin M, Liu W, Wang B. Intranasal Vaccination With Multiple Virulence Factors Promotes Mucosal Clearance of Streptococcus suis Across Serotypes and Protects Against Meningitis in Mice. J Infect Dis 2019;220(10):1679-1687. doi: 10.1093/infdis/jiz352.

16. Yoon JH, Jin H, Kim HJ, Hong SP, Yang MJ, Ahn JH, et al. Nasopharyngeal lymphatic plexus is a hub for cerebrospinal fluid drainage. Nature. 2024;625:768-777. doi: 10.1038/s41586-023-06899-4.

17. Spera I, Cousin N, Ries M, Kedracka A, Castillo A, Aleandri S, et al. Open pathways for cerebrospinal fluid outflow at the cribriform plate along the olfactory nerves. EBioMedicine. 2023;91:104558. doi: 10.1016/j.ebiom.2023.104558.
18. Arends JP, Zanen HC. Meningitis caused by Streptococcus suis in humans. Rev Infect Dis. 1988;10(1):131-137. doi: 10.1093/clinids/10.1.131.
19. Meng F, Wu NH, Nerlich A, Herrler G, Valentin-Weigand P, Seitz M. Dynamic Virus-Bacterium Interactions in a Porcine Precision-Cut Lung Slice Coinfection Model: Swine Influenza Virus Paves the Way for Streptococcus suis Infection in a Two-Step Process. Infect Immun. 2015;83(7):2806-2815. doi: 10.1128/IAI.00171-15.
20. Meng F, Wu NH, Nerlich A, Herrler G, Valentin-Weigand P, Seitz M, et al. Dynamic Virus-Bacterium Interactions in a Porcine Precision-Cut Lung Slice Coinfection Model: Swine Influenza Virus Paves the Way for Streptococcus suis Infection in a Two-Step Process. Infect Immun. 2015;83(7): 2806-15. doi: 10.1128/IAI.00171-15.
21. Meng F, Tong J, Vötsch D, Peng JY, Cai X, Willenborg M, et al. Viral Coinfection Replaces Effects of Suilysin on Streptococcus suis Adherence to and Invasion of Respiratory Epithelial Cells Grown under Air-Liquid Interface Conditions. Infect Immun. 2019;87(8):e00350-19. doi: 10.1128/IAI.00350-19.
22. Wu NH, Meng F, Seitz M, Valentin-Weigand P, Herrler G. Sialic acid-dependent interactions between influenza viruses and Streptococcus suis affect the infection of porcine tracheal cells. J Gen Virol. 2015;96(9):2557-2568. doi: 10.1099/jgv.0.000223.
23. Berthelot-Hérault F, Cariolet R, Labbé A, Gottschalk M, Cardinal JY, Kobisch M. Experimental infection of specific pathogen free piglets with French strains of

Streptococcus suis capsular type 2. Can J Vet Res. 2001; 65:196-200.

24. Berthelot-Hérault F, Gottschalk M, Morvan H, Kobisch M. Dilemma of virulence of Streptococcus suis: Canadian isolate 89-1591 characterized as a virulent strain using a standardized experimental model in pigs. Can J Vet Res. 2005;69:236-240.

25. Cao M, Feng Y, Wang C, Zheng F, Li M, Liao H, et al. Functional definition of LuxS, an autoinducer-2 (AI-2) synthase and its role in full virulence of Streptococcus suis serotype 2. J Microbiol. 2011;49(6):1000-11. doi: 10.1007/s12275-011-1523-1.

26. Shuster B, Khemmani M, Nakaya Y, Holland G, Iwamoto K, Abe K, et al. Expansion of the Spore Surface Polysaccharide Layer in Bacillus subtilis by Deletion of Genes Encoding Glycosyltransferases and Glucose Modification Enzymes. J Bacteriol. 2019;201(19):e00321-19. doi: 10.1128/JB.00321-19.

27. Yang XP, Fu JY, Yang RC, Liu WT, Zhang T, Yang B, et al. EGFR transactivation contributes to neuroinflammation in Streptococcus suis meningitis. J Neuroinflammation. 2016;13(1):274. doi: 10.1186/s12974-016-0734-0.

28. Li N, Ren A, Wang X, Fan X, Zhao Y, Gao GF, et al. Influenza viral neuraminidase primes bacterial coinfection through TGF-β-mediated expression of host cell receptors. Proc Natl Acad Sci U S A. 2015;112(1):238-43. doi: 10.1073/pnas.1414422112.

29. Pian Y, Gan S, Wang S, Guo J, Wang P, Zheng Y, Cai X, Jiang Y, Yuan Y. Fhb, a novel factor H-binding surface protein, contributes to the antiphagocytic ability and virulence of Streptococcus suis. Infect Immun. 2012;80(7):2402-13. doi: 10.1128/IAI.06294-11.

30. Bojarska A, Janas K, Pejsak Z, Otulak-Kozieł K, Garbaczewska G, Hryniewicz W, et al. Diversity of serotypes and new cps loci variants among Streptococcus suis isolates

from pigs in Poland and Belarus. Vet Microbiol. 2020;240:108534. doi: 10.1016/j.vetmic.2019.108534.

31. Pägelow D, Chhatbar C, Beineke A, Liu X, Nerlich A, van Vorst K, et al. The olfactory epithelium as a port of entry in neonatal neurolisteriosis. Nat Commun. 2018;9:4269. doi: 10.1038/s41467-018-06668-2.